ERF
European Rotorcraft Forum

A non-linear unsteady vortex lattice method for aeroelastic rotor loads evaluation

Alessandro Cocco*, Andrea Colli, Alberto Savino, Pierangelo Masarati, Alex Zanotti
Politecnico di Milano, Dipartimento di Scienze e Tecnologie Aerospaziali,
via La Masa 34, 20156, Milano - Italy
* alessandro.cocco@polimi.it

Abstract
The present work aims to extend the capabilities of DUST, a mid-fidelity aerodynamic solver developed at Politecnico di Milano, for the aerodynamic simulation of flight conditions characterised by flow separations. With this aim, a novel numerical element was implemented in the solver obtained by a coupling between the potential unsteady vortex lattice method and viscous aerodynamic data of airfoil sections available from two-dimensional high-fidelity CFD simulations or experimental wind-tunnel tests. The paper describes the mathematical formulation of the method and the results of a comprehensive validation of the novel numerical element performed by comparison with both high-fidelity CFD simulations results and experimental data. In particular the validation test cases included the evaluation of the airloads of a fixed rigid wing, the flutter speed of a wedged wing and the aerodynamic performance of the full scale proprotor of the XV-15 tiltrotor operating in hover condition, forward flight in helicopter mode and airplane mode.

1 Introduction

The study of the complex aerodynamics characterising the novel concept of electric take-off and landing aircraft (eVTOL) for Advanced Air Mobility (AAM) represents a challenge for computational fluid dynamics (CFD) tools. These kinds of flying machines experience a wide variety of flight conditions in which the rotor works with a high disk loading in helicopter mode, while a lower disk loading is experienced in airplane mode, where the rotor behave as a propeller. Currently, to obtain appreciable performance for both these flight conditions, the optimal design of eVTOL rotors leads to the use of highly twisted blades. Consequently, blades' airfoil sections experience a wide range of angles of attack that could overcome the stall condition, particularly in hovering.

In the preliminary design phase of innovative rotorcraft concepts as eVTOLs, a key aspect is to obtain a fast and accurate evaluation of aeroelastic loads on rotors and lifting surfaces. Indeed, as previously cited, the flight mission of these novel aircraft is characterised by different configurations, from hover to conversion phase and airplane mode. Thus, a huge number of simulations are required during their design phase to cover the entire aircraft flight envelope. Consequently, in recent years, the interest of industrial and scientific communities concerning the use of mid-fidelity aerodynamic solvers, based on vortex-particle method (VPM) for wake modelling [1, 2], has grown in the field of rotorcraft simulations. This interest was finalised to obtain fast and accurate numerical tools to be used in the preliminary design phase of novel rotorcraft architectures. Due to the lower computational costs required by mid-fidelity numerical methods with respect to high-fidelity CFD simulations based on Navier-Stokes solvers, these tools were also suitable to be coupled with structural solvers aimed to obtain a fast and accurate aeroelastic solution for rotorcraft configurations [3]. Nevertheless, the numerical approach implemented in such aerodynamic solvers presents some limitations, particularly concerning the evaluation of the aerodynamic performance in flight conditions characterised by consistent flow separations.

The present work describes a novel numerical element implemented in DUST [4], a mid-fidelity aerodynamic solver developed at Politecnico di Milano, to extend the code capabilities for the simulation of flight conditions characterised by important viscous effects. In particular, the novel numerical element is based on a coupling between the potential unsteady vortex lattice method and viscous aerodynamic data of airfoil sections available from two-dimensional high-fidelity CFD simulations (RANS) or experimental data. The paper includes a brief description of the state-of-the-art numerical elements implemented in DUST followed by the description of the mathematical formulation of the novel non-linear vortex lattice method (NL-VL). Moreover, the paper presents the validation of the novel method based on comparison of DUST simulations results with high-fidelity CFD and experimental data obtained over both fixed-wing and rotary-wing test cases.

2 Formulation of the DUST code

The mid-fidelity open-source software DUST has been developed from Politecnico di Milano since 2017 for the sim-

Presented at the 48th European Rotorcraft Forum, Winterthur, Switzerland, 6-8 September, 2022

ulation of the interactional aerodynamics of rotorcraft and unconventional aircraft configurations [4]. The code is released under the open source MIT license (`https://www.dust-project.org/`). The capabilities of the code have been quite extended in recent years and DUST has been also coupled to the open-source multibody solver MBDyn [3], also developed at Politecnico di Milano, enabling to perform aeroelastic analysis of complete rotorcraft configurations. The mathematical formulation of DUST relies on an integral boundary element formulation of the aerodynamic problem and vortex-particle modelling [1, 2] of the wakes. This choice naturally fits the Helmholtz decomposition of the velocity field from a mathematical point of view and avoids the numerical instabilities occurring with connected models of the wake. A model can be composed of several components, connected to user-defined reference frames, whose position and motion can be defined in a hierarchical way. The presence of different aerodynamic elements allows for different levels of fidelity in the model, ranging from lifting line elements to zero-thickness lifting surfaces and surface panels for thick solid bodies.

The lifting line (LL) element implemented in DUST is a 1-D model of thin slender lifting bodies, whose sectional aerodynamic coefficients of lift, drag, and pitching moment, i.e. c_l, c_d, c_m, are provided as a function of the local angle of attack α, the local Reynolds number Re and the local Mach number M. This allows taking into account the airfoil camber and thickness and both viscous and compressibility effects on aerodynamic loads computation. However, since the problem is stated in explicit form, numerical instability may occur during aerodynamic or aeroelastic analysis. The vortex lattice (VL) method provides the aerodynamic elements for the discrete representation of the mean surface of thin lifting bodies, modeled as a sheet of vortex rings of intensity Γ equivalent to a piecewise-uniform surface doublet distribution. The compressibility effects are taken into consideration by applying a Prandtl-Glauert correction on the loads, while the element is not able to capture the nonlinear behavior of the aerodynamic loads. The element relies on a fully implicit numerical scheme that provides numerical stability. The surface panels (SP) are formulated as a Morino-like problem [5] in implicit form. With this element, the real shape of the component can be described by applying the non-penetration boundary condition in the physical position. However, this element is not able to capture the nonlinear effect on the aerodynamic loads.

The main peculiarities of the aerodynamic elements implemented in DUST are reported in Table 1, while the complete mathematical formulation of the code is described in [4].

	Lifting Line (LL)	Vortex Lattice (VL)	Non-Linear VL (NL-VL)	Surface Panel (SP)
3D Unsteady	Yes	Yes	Yes	Yes
Thickness	Yes (Via database)	No	Yes (Via database)	Yes
Camber	Yes (Via database)	Yes	Yes	Yes
Viscous effects	Yes (Via database)	No	Yes (Via database)	No
Compressibility	Yes (Via database)	Yes (Via correction)	Yes (Via database)	Yes (Via correction)
Physical shape	No	No	No	Yes
Numerical scheme	Explicit	Implicit	Implicit	Implicit
Computational cost	Low	Low	Medium	High

Table 1: Summary of DUST available components and their characteristics

2.1 Non-Linear Vortex Lattice method

To overcome both limitations of LL (due to numerical scheme) and VL (related to viscous effects capturing), the two elements were joined together providing a new nonlinear vortex lattice element. In the first step, the potential solution of the linear vortex lattice is calculated, by solving the linear system that impose the non penetration boundary condition on the vortex lattice panel:

$$\hat{\mathbf{n}} \cdot \mathbf{u}_\phi = \hat{\mathbf{n}} \cdot \left(\mathbf{u}_b - \mathbf{U}_\infty - \mathbf{u}_\psi \right) \tag{1}$$

where $\mathbf{u}_\phi$ is the potential velocity, $\mathbf{u}_b$ is the body velocity, $\mathbf{U}_\infty$ is the free-stream velocity $\mathbf{u}_\psi$ is the rotational perturbation velocity. In the vortex lattice method, the surface is discretized as sheet of vortex wing of intensity Γ_{i_v}, equivalent to a piecewise-uniform surface doublet distribution with the same intensity μ_{i_v}. The boundary condition is written for each panel collocation point and we can rewrite the problem in a linear system form:

$$\mathbf{A}\Gamma = \mathrm{RHS} \tag{2}$$

Where each term a_{ij} of matrix $\mathbf{A}$ is defined as the velocity component induced by unit strength Γ_i, normal to the surface at collocation point i. After the solution of the system, it is possible to calculate the angle of attack of each stripe in the component as for the lifting line case. Then, a fixed point iterative problem is solved, as for the LL case, by imposing a convergence between the lift coefficient derived from the aerodynamic look-up table and the one calculated from the stripe intensity. For each iteration, the vortex lattice linear system is solved by modifying only the right-hand side and taking as results the updated circulations. To numerically stabilize the method two kind of relaxation are available:

- Constant relaxation, where the updated right-hand

side of the system is:

$$\mathrm{RHS}_i = \mathrm{RHS}_{i-1} + \alpha \cdot \mathbf{r} \tag{3}$$

where α is the constant relaxation factor, and $\mathbf{r}$ is the residual vector, defined as the difference between the lift coefficient solved from the linear system and the one obtained for the aerodynamic look-up table at iteration i.

- Aitken acceleration [6], where the updated right-hand side of the system is

$$\alpha_i = -\alpha_{i-1} \frac{\mathbf{r}_{i-1} \cdot \Delta\mathbf{r}_i}{\Delta\mathbf{r}_i \cdot \Delta\mathbf{r}_i} \tag{4}$$

where α_i is the Aitken relaxation factor for iteration i, and $\mathbf{r}$ is the residual vector and $\Delta\mathbf{r}_i$ is the difference the residuals at iteration i and $i-1$. Then the RHS is updated as described in eq. 3.

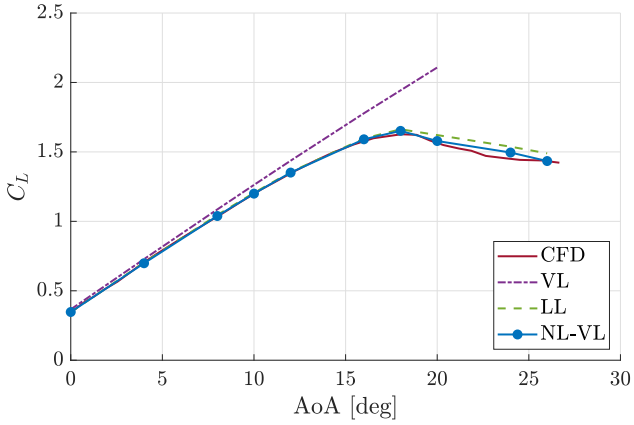

Figure 1: Comparison of the NACA 4415 wing lift coefficient (C_L) as function of angle of attack: high-fidelity CFD simulations results from [7] (CFD), DUST vortex lattice (VL), lifting line (LL) and non-linear vortex lattice (NL-VL) simulations results.

3 Results and Discussion

The present section describes the results of the validation of the novel numerical approach tested on both fixed-wing and rotary-wing benchmark cases available from literature for aerodynamic and aeroelastic problems.

3.1 Rigid Fixed-Wing

Firstly, a simple finite wing benchmark case is considered to test the correct implementation of the method. In particular, the test case consists of a rectangular wing with an aspect ratio equal to 12, a constant chord of $1\,\mathrm{m}$ and a constant NACA 4415 airfoil section. Figure 1 shows the comparison of the wing lift coefficient as a function of the angle of attack computed by high-fidelity CFD simulations from Hosangadi et al. [7]) and by DUST using both the already implemented LL and VL elements and the novel non-linear vortex lattice method (NL-VL). The effectiveness of the non-linear vortex-lattice method is evident, as shown by the remarkable agreement with the curves obtained using the lifting-line approach implemented in DUST and with high-fidelity CFD simulations, both considering viscous contributions for airloads evaluation. This result confirms the correctness of the novel implementation based on the integration of the viscous aerodynamic 2D data and shows the capabilities of the method to capture stalled and post-stalled conditions with respect to the purely potential VL model.

3.2 Goland's Wing Flutter

Secondly, an aeroelastic benchmark test is considered, i.e. the Goland's wing [8]. This test case was widely used in literature to validate aeroelastic codes. The study of this low-aspect-ratio wedged wing with aspect ratio ≈ 3.33 is also of interest because it highlights the effect of using a 2D or a 3D aerodynamic model on flutter computation. This aeroelastic model was investigated in a previous work by Savino et al. [3] by using the coupled DUST-MBDyn code, extended in the present activity including the use of the non-linear vortex lattice method for the evaluation of the wing flutter. In particular, to study the flutter instability, a non-zero angle of attack of $0.05°$ was introduced as a perturbation, as done in [9]. The frequency and damping of the model response were identified from the time history of the wing-tip deflection using the matrix pencil estimation (MPE) method [10]. Table 2 reports a comparison of the flutter speed and frequency computed by several authors for this test case. Results from the coupled DUST-MBDyn code are in quite good agreement with those obtained by similar codes using 3D aerodynamic models [11, 12, 9], confirming the suitability of the novel approach for aeroelastic simulations. In details, the discrepancy with the results obtained with the same multibody structural model, but using its built-in aerodynamic model based on two-dimensional unsteady strip theory, indicates the higher capability of the coupled code for the investigation of aeroelastic problems.

Author	*Model*	V_f [m s^{-1}]	f_f [Hz]
Goland [8]	Analytical (2D)	137.2	11.25
Patil et al. [11]	Strip Theory	135.6	11.17
Wang et al. [12]	ZAERO	174.3	-
Wang et al. [12]	UVLM	163.8	-
Murua et al. [9]	SHARP UVLM	165	10.98
Savino et al. [3]	MBDyn's strip theory	135.1	11.07
Savino et al. [3]	DUST (VL)-MBDyn	168.2	10.84
Savino et al. [3]	DUST (SP)-MBDyn	174.2	11.06
Present work	DUST (NL-VL)-MBDyn	171.4	10.97

Table 2: Comparison of flutter speed and frequency computed for Goland's wing.

In order to evaluate the capabilities of the coupled code DUST-MBDyn using the different aerodynamic models including the novel NL-VL approach, Fig. 3 presents the computed damping of the first beam torsional mode of the wing as functions of the free-stream speed.

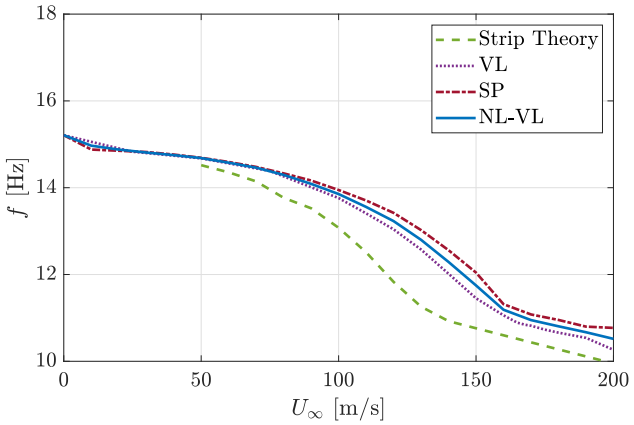

Figure 2: Frequency f of the first torsional modes vs speed U_∞ for Goland's wing. Coupled DUST-MBDyn simulations results (VL, NL-VL and SP mesh) and MBDyn results with 2D strip theory aerodynamic model.

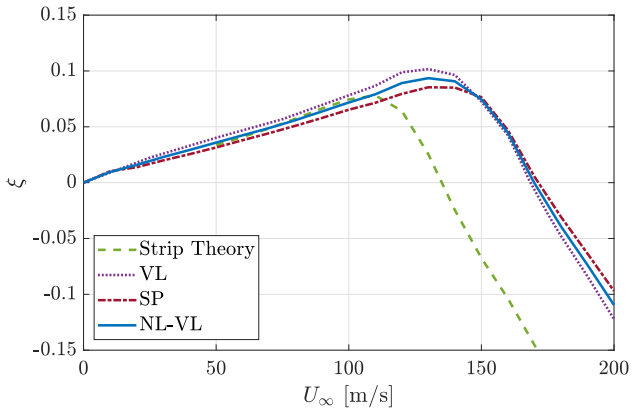

Figure 3: Damping (ξ) of the first torsional modes vs speed U_∞ for Goland's wing. Coupled DUST-MBDyn simulations results (VL, NL-VL and SP mesh) and MBDyn results with 2D strip theory aerodynamic model.

Numerical results of the coupled simulations obtained using a panel mesh (SP) show a slightly higher aerodynamic damping than those obtained using both VL approaches. An increase in the predicted flutter speed of approximately $3.7\,\%$ is observed. Given these minor differences in the results obtained with the two models, a vortex lattice mesh appears to be more convenient than a surface panel one, as the computational cost reduces significantly with no loss in accuracy, at least for simple configurations without complex aerodynamic interaction between bodies.

3.3 XV-15 Proprotor

A third benchmark case, this time in rotorcraft field, is considered in the present work, consisting in the simulation of the proprotor of the XV-15 tiltrotor with metal blades in different flight conditions, i.e. hover condition, forward flight in helicopter mode, and airplane mode.

For the present test case, the three propeller blades were modeled as rigid blades using non-linear vortex lattice elements only. The tabulated aerodynamic performances of the propeller airfoils were taken from [13]. DUST simulations were performed considering a length of 10 propeller revolutions with a time discretisation of $5°$ of blade azimuthal angle. The computational time required to complete the simulation of the rotor configuration was about 8 minutes using a workstation with a Dual Intel Xeon Gold 6230R @2.10Ghz with 104 cores processor.

In the following, DUST simulations results obtained using the NL-VL approach are compared to the recent high-fidelity numerical simulations results obtained by Jia et al. [14] using a Detached Eddy Simulation (DES) approach and to the experimental data collected in the test campaigns described by Felker et al. [13] and Betzina [15].

3.3.1 Hover flight condition

Figures 4 and 5 show the comparison of the rotor thrust coefficient (C_T) as a function, respectively, of the blade collective angle and of the rotor torque coefficient(C_Q), while Fig. 6 shows the comparison of the rotor figure of merit (FM).

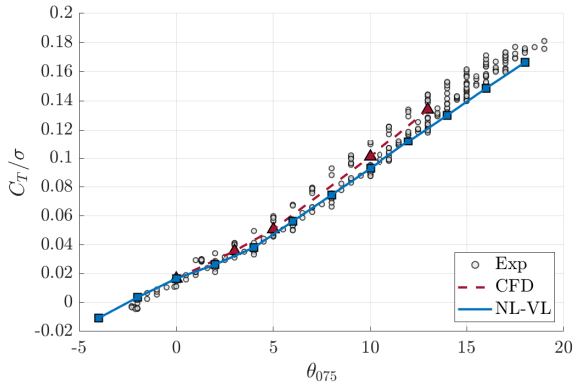

Figure 4: Comparison of the C_T/σ vs collective angle for the XV-15 proprotor in hover. Experimental data taken from [13] (Exp), numerical data from [14] (CFD) and DUST (NL-VL).

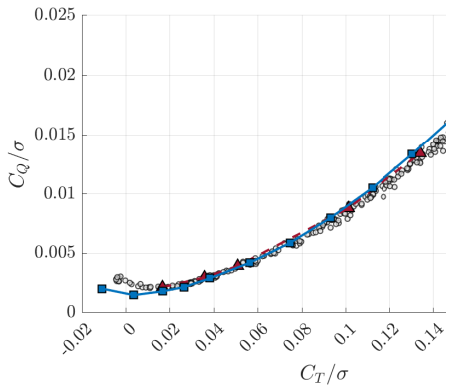

Figure 5: Comparison of the C_Q/σ vs C_T/σ for tor in hover. Experimental data taken from [13 data from [14] (CFD) and DUST (NL-VL).

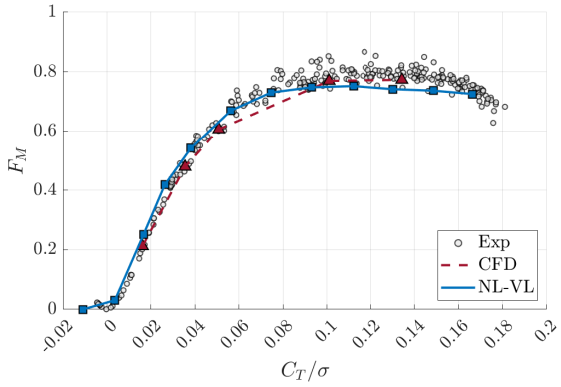

Figure 6: Comparison of the F_M vs C_T/σ for the XV-15 proprotor in hover. Experimental data taken from [13] (Exp), numerical data from [14] (CFD) and DUST (NL-VL).

The performance curves obtained with DUST resume quite well the behaviour of the experimental data in the whole range of blade collective angles tested. Moreover, the curves comparison shows that DUST approach provides similar capabilities to a DES approach in terms of aerodynamic performance evaluation for such a case, but requiring a quite lower amount of computational effort. In particular, the rotor figure of merit comparison shown in Fig. 6, clearly indicates the very good agreement with experiments of the overall rotor performance in hover calculated by DUST, particularly at low C_T/σ. Moreover, the quite lower computational cost required by DUST approach enabled to perform a quite higher amount of simulations with respect to high-fidelity CFD, thus covering with a finer step of collective angle the whole operational range described by the experimental curve.

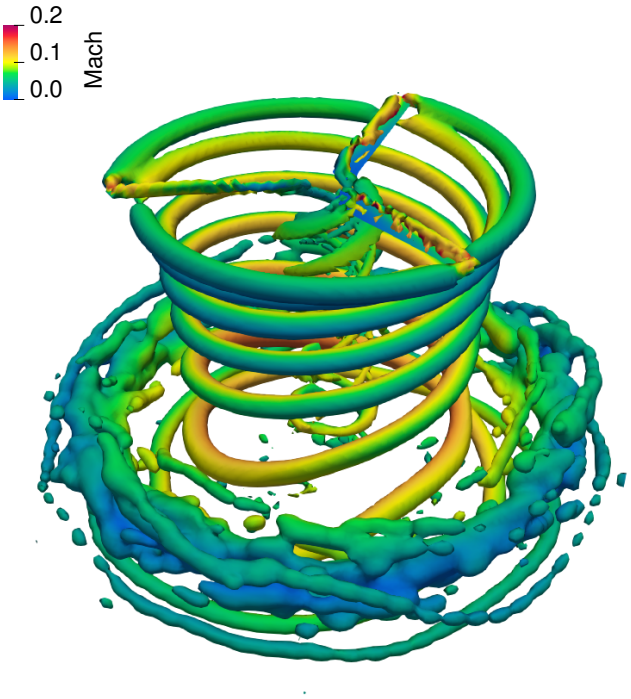

Figure 7: Wake visualization of the XV-15 proprotor in hover by means of iso-surfaces of Q-criterion computed by DUST colored by Mach number.

A flow field representation of the present test condition is presented in Fig. 7, showing the helical vortical structure of the proprotor wake in hover computed by DUST highlighted by the iso-surfaces of Q-criterion.

3.3.2 Forward flight condition

In forward flight condition, helicopter mode configurations of the XV-15 proprotor were investigated with DUST considering three shaft angle attitudes, i.e. $\alpha = -5°$, $\alpha = 0°$ and $\alpha = 5°$, at advance ratio 0.17. This choice enabled, analogously to what done in [14], to investigate DUST capabilities in both propulsive and descending forward flight conditions.

Figures 8 and 9 show the comparison of the rotor torque coefficient (C_Q) as a function, respectively, of the rotor thrust coefficient(C_T) and of the lift coefficient (C_L).

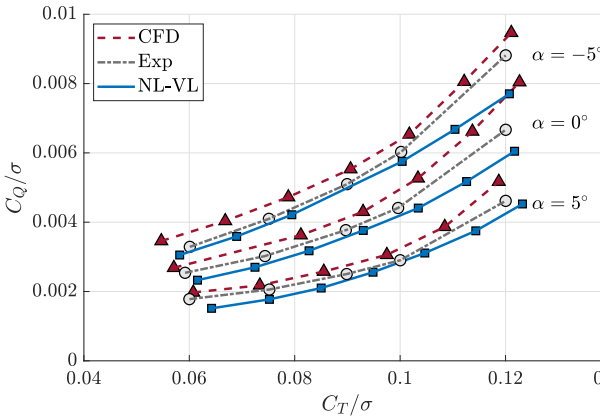

Figure 8: Comparison of the C_Q/σ vs C_T/σ for the XV-15 p protor in forward flight. Experimental data taken from [15] (Ex numerical data from [14] (CFD) and DUST (NL-VL).

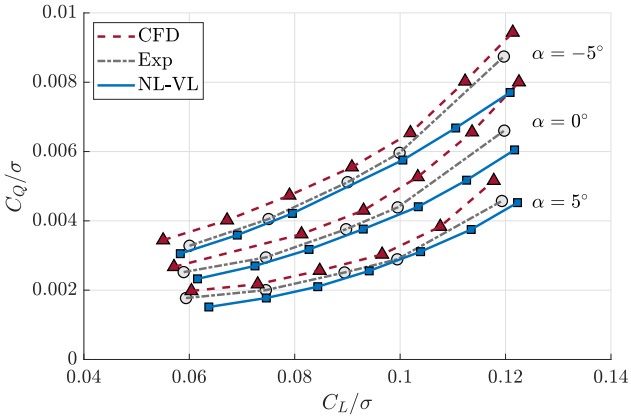

Figure 9: Comparison of the C_Q/σ vs C_L/σ for the XV-15 proprotor in forward flight. Experimental data taken from [15] (Exp), numerical data from [14] (CFD) and DUST (NL-VL).

A quite good agreement with experiments is found also for this flight condition for the proprotor aerodynamic performance calculated by DUST. In particular, DUST results slightly underestimate the experimental performance curves in the whole range of collective blade angles considered. Nevertheless, the discrepancies of DUST results from experimental data are relatively lower with respect to CFD simulations results, particularly in the lower range of collective angles tested. On the other hand, at higher thrust or lift coefficient range, larger discrepancies with respect to experimental data are found for DUST representation of the proprotor aerodynamic performance. This behaviour could be related to the limitation of DUST approach to reproduce accurately high blade loading conditions characterised by more important viscous effects and separated flow regions.

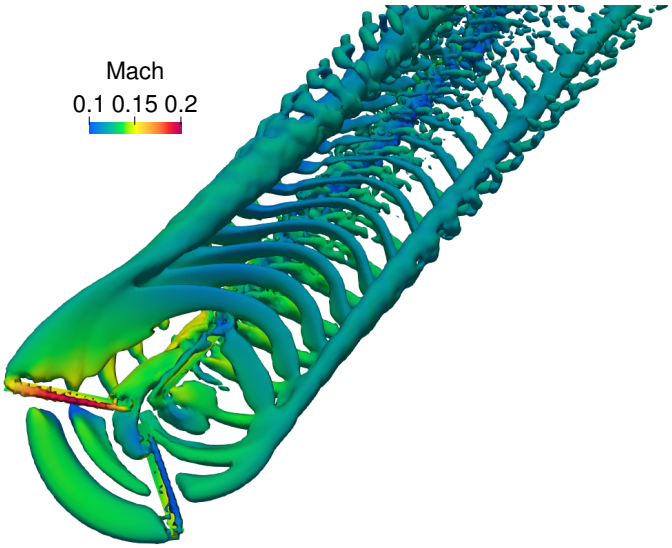

Figure 10: Wake visualization of the XV-15 proprotor in advanced flight at 5° collective, and $\alpha = 5°$ by means of iso-surfaces of Q-criterion computed by DUST colored by Mach number.

Indeed, these flight conditions are also characterised by consistent aerodynamic interactional effects, as shown by the flow visualization presented in Fig. 10 highlighting the interaction of the tip vortices with the downstream blades.

3.3.3 Airplane Mode flight condition

Airplane mode configurations of the XV-15 proprotor were simulated using DUST at advance ratio 0.337 for different collective blade pitch angles. The capabilities of DUST to reproduce the aerodynamic performance of the proprotor in this flight condition is evaluated by comparing the torque coefficient (C_Q) and propulsive efficiency (η) as function of the thrust coefficient (C_T), see respectively Figs. 11 and 12.

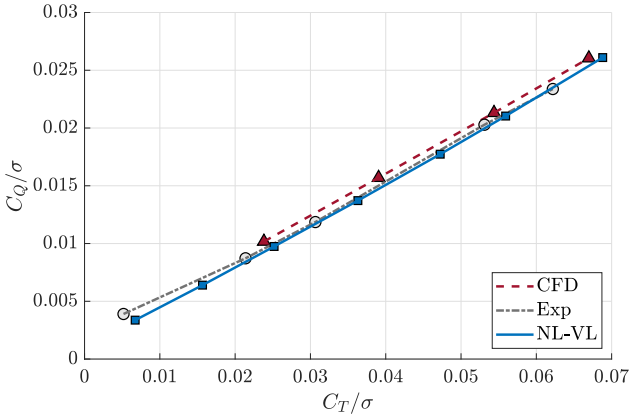

Figure 11: Comparison of the C_Q/σ vs C_T/σ for the XV-15 proprotor in airplane mode flight. Experimental data taken from [15] (Exp), numerical data from [14] (CFD) and DUST (NL-VL).

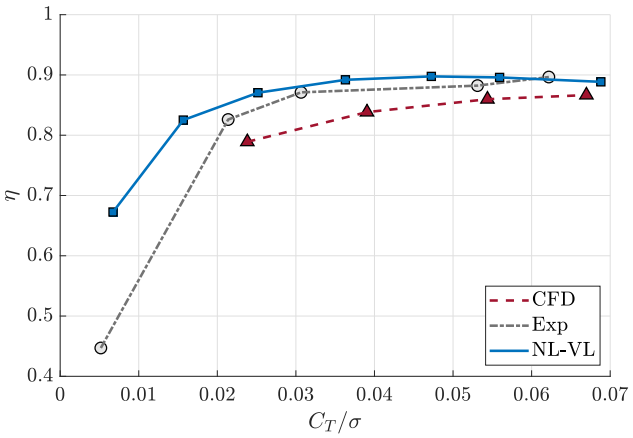

Figure 12: Comparison of the propulsive efficiency eta vs C_T/σ for the XV-15 proprotor in airplane mode flight. Experimental data taken from [15] (Exp), numerical data from [14] (CFD) and DUST (NL-VL).

A very good agreement between DUST simulations results and experimental data is found for this flight conditions. In particular, the discrepancies with respect to experimental curves exposed by DUST simulations results are quite lower with respect to the ones obtained by high-fidelity CFD simulations, thus confirming the suitability of DUST approach for an accurate evaluation of propellers aerodynamic performance. Indeed, a slight overestimation of the propulsive efficiency evaluated by experiments can be observed from DUST simulation results over almost the whole range of rotor thrust conditions tested, while a higher discrepancy in the order of 20% is found only for the lowest blade loading condition tested.

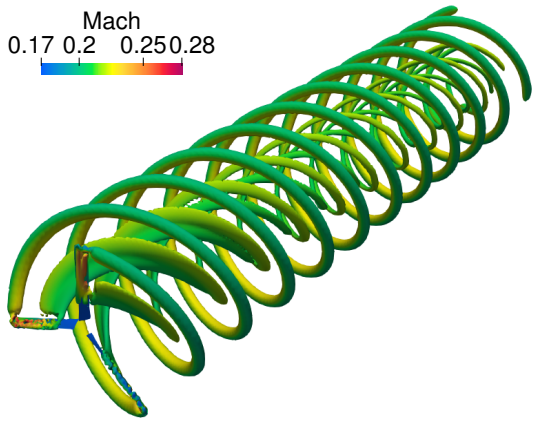

Figure 13: Wake visualization of the XV-15 proprotor in airplane mode by means of iso-surfaces of Q-criterion computed by DUST colored by Mach number.

The flow field representation of an airplane mode flight condition computed by DUST is shown in Fig. 13 by means of iso-surfaces of Q-criterion, highlighting a quite coherent helical vortical structure of the proprotor wake without interactions due to the free-stream velocity dragging characterising this flight condition.

4 Conclusions

A novel non-linear vortex lattice element was implemented in the mid-fidelity aerodynamic code DUST. The aim of the novel method is to overcome the limitations of the state-of-the-art already implemented numerical elements, i.e. lifting lines and classical vortex lattice elements, related, respectively, to the occurrence of numerical instabilities and to the inability to capture viscous effects. The novel numerical method was validated and tested against different test cases ranging from fixed-wing to rotorcraft applications.

The comparison with experimental results obtained for a steady fixed-wing test case showed that DUST simulations performed using this novel approach allowed great accuracy in capturing the wing aerodynamic performance, also for stalled conditions. Moreover, aeroelastic simulations performed with DUST over a wedged fixed-wing confirmed the capabilities of the novel approach to capture flutter speed without any loss of accuracy with respect to classical surface panels or vortex lattice methods.

DUST simulations results performed over the XV-15 proprotor showed a very good agreement with experimental data for different flight conditions ranging from hover to airplane mode. In particular, DUST simulations results showed the capability to obtain a similar degree of accuracy in terms of rotor aerodynamic performance with respect to high-fidelity CFD approach, but at a quite lower computational cost. This result further highlighted the potentialities of the implemented approach for the design and investigation of rotorcraft configurations.

Copyright Statement

References

[1] G. S. Winckelmans. *Topics in vortex methods for the computation of three-and two-dimensional incompressible unsteady flows*. Ph.D. dissertation, California Institute of Technology, 1989.

[2] G. H. Cottet and P. D. Koumoutsakos. *Vortex methods: theory and practice*. Cambridge University Press, 2000.

[3] Alberto Savino, Alessandro Cocco, Alex Zanotti, Matteo Tugnoli, Pierangelo Masarati, and Vincenzo Muscarello. Coupling mid-fidelity aerodynamics and multibody dynamics for the aeroelastic analysis of rotary-wing vehicles. *Energies*, 14(21):6979, 2021.

[4] Matteo Tugnoli, Davide Montagnani, Monica Syal, Giovanni Droandi, and Alex Zanotti. Mid-fidelity approach to aerodynamic simulations of unconventional vtol aircraft configurations. *Aerospace Science and Technology*, 115:106804, 2021.

[5] L. Morino and C.-C. Kuot. Subsonic potential aerodynamics for complex configurations: A general theory. *AIAA Journal*, 12(2):191–197, 1974. doi:10.2514/3.49191.

[6] Ulrich Küttler and Wolfgang A Wall. Fixed-point fluid-structure interaction solvers with dynamic relaxation. *Computational mechanics*, 43(1):61–72, 2008.

[7] Justin L Petrilli, Ryan C Paul, Ashok Gopalarathnam, and Neal T Frink. A CFD database for airfoils and wings at post-stall angles of attack. In *31st AIAA applied aerodynamics conference*, page 2916, 2013.

[8] Martin Goland. The flutter of a uniform cantilever wing. *Journal of Applied Mechanics-Transactions of the Asme*, 12(4):A197–A208, 1945.

[9] Joseba Murua, Rafael Palacios, and J Michael R Graham. Assessment of wake-tail interference effects on the dynamics of flexible aircraft. *AIAA Journal*, 50(7):1575–1585, 2012.

[10] Yingbo Hua and Tapan K Sarkar. Matrix pencil method for estimating parameters of exponentially damped/undamped sinusoids in noise. *IEEE Transactions on Acoustics, Speech, and Signal Processing*, 38(5):814–824, 1990.

[11] Mayuresh J Patil, Dewey H Hodges, and Carlos ES Cesnik. Nonlinear aeroelastic analysis of complete aircraft in subsonic flow. *Journal of Aircraft*, 37(5):753–760, 2000.

[12] Zhicun Wang, PC Chen, DD Liu, DT Mook, and MJ Patil. Time domain nonlinear aeroelastic analysis for HALE wings. In *47th AIAA/ASME/ASCE/AHS/ASC Structures, Structural Dynamics, and Materials Conference 14th AIAA/ASME/AHS Adaptive Structures Conference 7th*, page 1640, 2006.

[13] David B. Signor Fort F. Felker, Mark D. Betzina. Performance and loads data from a hover test of a full-scale XV-15 rotor. Technical report, NASA Ames Research Center, Moffett Field California, 1985.

[14] Feilin Jia, John Moore, and Qiqi Wang. Assessment of detached eddy simulation and sliding mesh interface in predicting tiltrotor performance in helicopter and airplane modes. In *AIAA AVIATION 2021 FORUM*, page 2601, 2021.

[15] Mark D Betzina. Rotor performance of an isolated full-scale xv-15 tiltrotor in helicopter mode. Technical report, NATIONAL AERONAUTICS AND SPACE ADMINISTRATION MOFFETT FIELD CA ROTORCRAFT, 2002.